World Journal of Advanced Engineering Technology and Sciences
eISSN: 2582-8266
Cross Ref DOI: 10.30574/wjaets
Journal homepage: https://wjaets.com/

(RESEARCH ARTICLE)

Check for updates

Flow of tiny particles past a cylinder: A COMSOL multi-physics analysis

Bijoy Kumar Deb * and Rahul Deb

Department of Mechanical Engineering, Tripura Institute of Technology Agartala, Tripura, 799015, India.

World Journal of Advanced Engineering Technology and Sciences, 2025, 17(02), 028-038

Publication history: Received on 26 September 2025; revised on 02 November 2025; accepted on 04 November 2025

Article DOI: https://doi.org/10.30574/wjaets.2025.17.2.1463

Abstract

This study investigates the flow of tiny particles past a circular cylinder using COMSOL Multiphysics 6.1, focusing on laminar and transitional regimes in a two-dimensional channel. Comprehensive numerical simulations were performed to analyze the interaction between the fluid field and particle trajectories, with geometry, material properties, and boundary conditions systematically defined for accuracy. The methodology involved parameter definition, domain meshing with finer elements, and time-dependent analyses of drag and lift coefficients, alongside detailed particle tracking. Results revealed temporal variations in drag coefficient dependent on flow stability, and highlighted boundary layer behavior, including separation phenomena. Continuous monitoring of vortex shedding and wake structure provided insights into the complex dynamics governing particle transport near the cylinder. The findings underscore the significance of computational modeling for understanding fluid-particle interactions and demonstrate that particle dynamics and drag forces are highly sensitive to flow regime and system configuration. This research contributes to the improved prediction of particulate movement in engineering systems, offering a validated multiphysics framework for future studies in flow control and design optimization.

Keywords: Particle-fluid interaction; Vortex shedding; Drag and lift coefficients; COMSOL Multiphysics; Laminar flow

1. Introduction

The study of fluid flow past a circular cylinder remains one of the most fundamental and widely explored problems in fluid mechanics. Owing to its direct relevance to engineering applications such as offshore structures, bridge piers, heat exchangers, and underwater cables, understanding the flow dynamics and wake formation behind a cylinder continues to attract considerable research interest [1, 2]. The unsteady flow behaviors, including vortex shedding and transitions between laminar and turbulent regimes, have served as benchmark scenarios for validating computational fluid dynamics (CFD) techniques. Numerical modeling tools such as COMSOL Multiphysics have expanded the scope of such studies by allowing coupled analyses of flow physics, surface deformation, and particle-fluid interactions at multiple scales [3].

Classical investigations demonstrated that the wake behind a circular cylinder evolves from steady laminar to periodic vortex shedding as the Reynolds number increases. Braza et al. [4] examined two-dimensional laminar flow past a circular cylinder and described the emergence of the von Kármán vortex street and its transition from steady to irregular flow behavior. Building upon these foundational results, Rodi [5] explored turbulence modeling for realistic flow configurations, improving the predictive capability of CFD simulations. Studies on surface roughness and irregularities, such as those by Achenbach and Heinecke [6], revealed significant modifications in drag and flow transition characteristics. Williamson [7] provided detailed experimental correlations of Strouhal numbers with Reynolds numbers, establishing baselines for wake dynamics that have since guided numerous numerical validations, including those by Norberg and Zdravkovich [8]. Sheridan et al. [9] classified near-wake structures in submerged cylinder flows, identifying key vorticity layers and localized wave breaking at the free surface. Similarly, Barkley and

* Corresponding author: Bijoy Kumar Deb. Email: bijoykrdb@gmail.com

Henderson [10] and Thompson et al. [11] advanced understanding of three-dimensional flow transition mechanisms using Floquet stability analysis and direct numerical simulation. Experimental works by Honji et al. [12] and numerical analyses by Reichl et al. [13] highlighted how surface deformation and vorticity transport significantly influence wake evolution. Subsequent studies by Gopalan and Katz [14] and Oshkai and Rockwell [15] deepened this understanding through detailed visualization of surface wave interactions and jet-like flows between vortex layers. Advancements in computational methods have allowed refined modeling of such complex interactions. Oliveira et al. [16] compared multiple CFD platforms to assess their reliability in simulating cylinder flow. Using large eddy simulations, Koo et al. [17] examined three-dimensional features and vorticity flux balance in the near wake, while Bouscasse et al. [18] employed smoothed particle hydrodynamics to capture free-surface deformation phenomena. Comprehensive synthesizing works by Lin et al. [19] and Lin and Rockwell [20] emphasized the importance of the coupling between surface dynamics and vortex generation. Parallel efforts by Nguyen et al. [21] and Rajani et al. [22] refined computational frameworks within COMSOL Multiphysics, focusing on mesh refinement and turbulence model accuracy. More recently, Kim et al. [23] and Cao et al. [24] advanced the understanding of surface-to-wake interactions, while emerging studies by Rashidi et al. [26] and Zhang et al. [27] introduced machine learning to predict flow separation and vorticity field evolution across diverse flow regimes.

Despite extensive research, the behavior of microscopic particles or dispersed phases within a flow past a cylinder, especially near deformable or partially free surfaces, remains insufficiently resolved. Most studies have concentrated on macroscopic vorticity and drag characteristics, often neglecting the micro-scale flow-particle coupling that is crucial for understanding particulate transport, sedimentation, or pollutant dispersion. Additionally, limited COMSOL-based analyses have explicitly examined multiphase or particle-laden flow past cylinders under varying Reynolds and Froude conditions.

This research aims to address these gaps by employing COMSOL Multiphysics to simulate and analyze the flow of tiny particles past a circular cylinder. The study focuses on coupling particle motion with underlying fluid dynamics to capture wake interaction, pressure distribution, and drag variation under laminar and transitional regimes. Specific objectives include (i) modeling two-dimensional flow fields around a cylinder with particle tracking; (ii) analyzing wake structures and vortex shedding patterns; and (iii) quantifying the effects of particle size and concentration on flow field characteristics. The outcomes of this study are expected to enhance the understanding of micro-scale hydrodynamics in confined geometries and support improved designs for flow and particle control in engineering systems.

2. Materials and Methods

2.1. COMSOL Multiphysics

This study employed COMSOL Multiphysics 6.1, a robust simulation platform renowned for its capability to model and analyze coupled physical phenomena relevant to engineering and scientific research. COMSOL's comprehensive suite includes:

- Multiphysics Simulation: The software efficiently models linked physical events, such as fluid flow, heat transfer, electromagnetics, and structural mechanics, vital for accurately capturing the complex nature of flow around obstacles.
- Physics Modules: Specialized modules for fluid dynamics are utilized to incorporate accurate representations of laminar and transitional flow.
- Graphical User Interface (GUI): COMSOL's GUI streamlines workflow—from geometry creation and meshing to assigning physical properties, applying boundary conditions, and visualizing simulation results—without the need for user coding.

By leveraging these features, the setup replicates realistic conditions of micro-particle transport past a cylinder and delivers high-fidelity numerical results.

2.2. Model Definition

The following model looks at an unstable, incompressible movement in a round cylinder positioned in a channel perpendicular to the incoming fluid flow to show the method for investigating these situations. Movement requires a bit of asymmetry to cause the vortex formation in the case of a symmetric input velocity profile. Setting the cylinder in place with a little counteract from the centre of the flow will accomplish this. It is challenging to forecast how long a simulation will take for a recurring flow pattern to emerge. The R_e number. is dependent on the diameter of the cylinder,

which is a vital indicator. The flow is constant for low numbers (less than 100). Although the von Karman vortex street has emerged in this simulation with a Reynolds number of 100, even yet, the flow is not entirely turbulent.

While Oscillations' Frequency & Amplitude are constant, flow specifics are mostly susceptible to changes. It may contrast the flowing animation captured during that moment with a very slight difference caused by different duration calculating resonance to get a sense of this delicateness. It's crucial to memorize as delicacies are not just numerical artefacts, but a physical reality. You can use the non-linear solution to evaluate and calculate the approach at a lower Reynolds number prior to computing the time fluctuating forces over the cylinder. Time duration will be less since basic flaws and errors may be there, and it will be resolved before the final time-dependent simulation, which takes a lot of work. The viscous forces operating on the cylinder surface are determined by the gradient of the velocity field at that location of the cylinder. Even though it's feasible, it is not particularly precise to evaluate the gradient of velocity at the border by simply setting the FEM Solution apart. When the velocity field is represented by second-order elements, the differentiation yields first-order polynomials. The viscous force integrals may be calculated using two reaction force operators, which is a considerably superior method. These integrals are similar to correct second-order viscous force integrals. Alternatively, the no-slip condition might impose on utilizing a pair of weak constraints. During computing essentials about reaction forces or flux after processing, it's preferable to utilize the operator for reaction force rather than weak constraints. Even more remarkable than the drag force and lift forces themselves are the dimensionless coefficients of these two phenomena.

2.3. Drag Coefficient

A dimensionless measurement called the drag coefficient (C_D) describes how difficult it is for an item traveling through a fluid (like water or air). It is a gauge of the object's ability to overcome fluid resistance. The drag coefficient is the ratio of the drag force to the product of dynamic pressure and reference point. The object's form has a significant impact on the drag coefficient. Compared to blunt or irregular forms, smooth and streamlined designs tend to disrupt the airflow less, thereby having lower drag coefficients. In domains like fluid dynamics, vehicle design, and aerodynamics, drag coefficients are essential. They are used by engineers to maximize efficiency and reduce drag in the construction of cars, houses, and other structures. Drag coefficients differ significantly based on the item. As an illustration:

A streamlined car may have a 0.25 to 0.35. The radius of a sphere is around 0.47.

About 1.2 is the area of a flat plate perpendicular to the flow. Computational-Fluid-Dynamics (CFD) simulations are frequently done for calculating drag coefficients. Engineers can forecast and improve an object's aerodynamic performance with the use of these techniques.

$$C_D = \frac{2F_D}{\rho U^2{}_{mean} A} \quad (1)$$

Where, F_D is *the* drag force, ρ is the Fluid Density, U_{mean} is the mean velocity, A is the projected area (product of thickness and diameter of cylinder).

2.4. Lift Coefficient

A dimensionless quantity known as the lift coefficient (CL) describes the lift produced by a wing or airfoil as it travels through a fluid, usually air. It is a basic aerodynamic parameter that is utilized in various domains where lift and aerodynamic forces are important, as well as in the analysis and design of aircraft. Lift Coefficient is the product of the object's lift force and the fluid flow's dynamic pressure, multiplied by the object's reference area. The shape of the wing, the Angle of Attack, and the Reynolds number are some of the variables that affect the lift coefficient. Lift coefficients are widely used in aerodynamic calculations by engineers and designers to forecast and improve aircraft performance, from calculating take-off and landing speeds to creating effective wings and control surfaces. When assessing an aircraft's lift capacity under various flying situations, the lift coefficient is essential. It has a direct impact on variables like maximum lift, stall speed, and overall aerodynamic efficiency. The lift coefficient is a tool used by aircraft designers to improve wing forms, optimize for certain flying situations (such as cruise, take-off, and landing), and guarantee stable flight performance in a variety of scenarios. It enables comparisons between various airfoil configurations and forms to determine which design is best for a certain application, whether it is military aircraft, commercial airliners, or even other fields. In conclusion, especially in the context of aviation and aerospace engineering, the lift coefficient is a fundamental aerodynamic parameter that is vital to the design, operation, and comprehension of the aerodynamics of objects moving through fluids.

$$C_L = \frac{2F_L}{\rho U^2{}_{mean} A} \quad (2)$$

Where, F_L is *the* lift force, ρ is the Fluid Density, U_{mean} is the mean velocity, A is the projected area (product of thickness and diameter of cylinder).

2.5. Navier-Stokes Equation

The basic equations in fluid dynamics that explain the movement of fluids (liquids and gases) are known as the "Navier-Stokes equations". In the 1800s, George Gabriel Stokes and Claude-Louis Navier created them. These mathematical expressions for the conservation of momentum for a fluid take into consideration both the viscous (related to frictional forces) and inertial (related to acceleration) aspects.

The Equations:

Continuity Equation:

$$\partial\rho/\partial t \; + \; \nabla.(\rho V) \; = 0 \tag{3}$$

With V being the velocity vector and ρ being the fluid density, this equation represents the conservation of mass.

Momentum Equation (Navier-Stokes Equation):-

$$\rho\,(\frac{\partial V}{\partial t} + V.\nabla V\,) \; = \; -\nabla p \; + \; \nabla.T \; + \; \rho\, f \tag{4}$$

Here, T represents the stress tensor, which includes viscous stresses, ρ is the density, p is pressure, and f denotes body forces.

Navier-Stokes equations apply to laminar flow past a cylinder, which happens at a lower R_e no. Laminar flow occurs when a fluid flows smoothly in layers with minimal mixing between them. The Navier-Stokes equations cannot be used for the laminar flow past a cylinder without boundary conditions. These include the far-field conditions, in which the flow remains undisturbed a considerable distance from the cylinder, and the no-slip condition at the cylinder's surface, in which the fluid speed is zero with respect to the cylinder surface. The formulas shed light on how vortices—like the von Kármán vortex street—form rear the cylinder and how drag forces are determined. Understanding the intricate flow patterns is aided by the straightforward derivation of vorticity in the flow field from solutions of the Navier-Stokes equations. Although it's difficult to find analytical solutions of Navier-Stokes equations for complex geometries like a cylinder, these equations are crucial for accurate prediction and understanding of flow behaviour in experimental studies and numerical simulations like computational fluid dynamics, or CFD.

2.6. Analysis Procedure

The simulation followed sequential steps, each designed to capture essential flow features and particle dynamics in a two-dimensional channel intersected by a cylinder:

2.7. Defining Parameters

Key geometric and flow parameters, including channel width, height, length, cylinder radius, and mean inflow velocity, were established at the outset. The inflow velocity was configured using a smoothed step function to allow velocity modulation. The input parameters were defined in Table 1.

Table 1 Input parameters.

Name	Expression	Value	Description
U_{mean}	1[m/s]	1 m/s	Mean inflow velocity
H	0.41[m]	0.41 m	Height
W	2.2[m]	2.2 m	Width
R	0.05[m]	0.05 m	Cylinder radius

2.8. Geometrical Modeling

Geometrical construction started in the Geometry toolbar, with rectangles and circles defined by their respective sizes and positions. Boolean and partition operations refined the interaction between the channel and cylinder, resulting in a channel with a centrally positioned cylindrical obstacle. Zoom and build operations were used for clarity and accuracy in defining the computational domain.

2.9. Specifying Fluid Properties

The fluid was set as an incompressible single-phase with properties shown in Table 2.

Table 2 Fluid properties

Property	Variable	Value	Unit	Property Group
Density	ρ	1	kg/m^3	Basic
Dynamic viscosity	μ	1e-3	Pa·s	Basic

2.10. Meshing

The channel and cylinder domains were discretized using a physics-controlled mesh, with mesh element size set to "finer" for greater solution accuracy, especially near boundary layers and the cylinder surface.

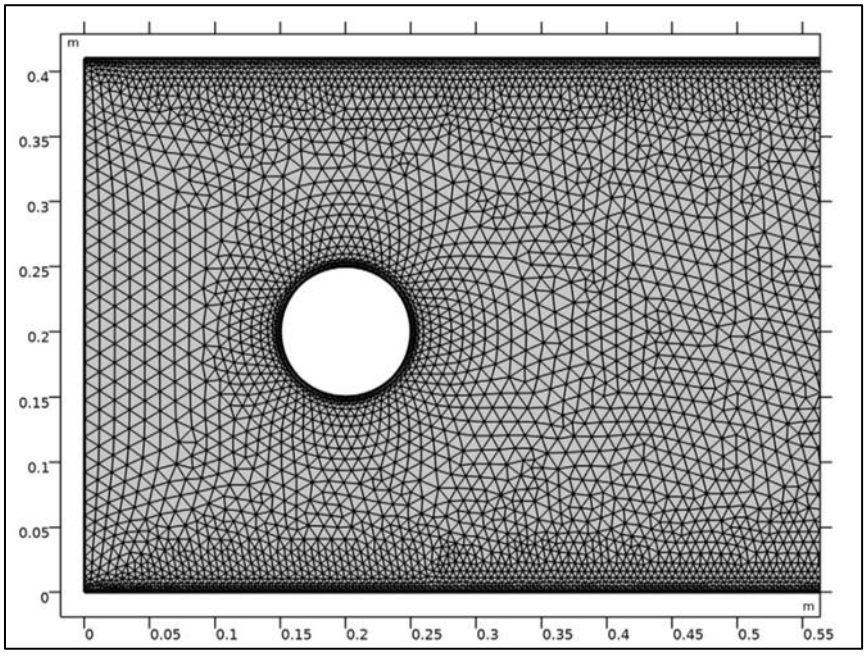

Figure 1 Boundary layer on the inlet of cylinder given by Physics controlled mesh

The boundary layer on the inlet of the cylinder, given by a physics-controlled mesh, is depicted in Figure 1

2.11. Solution & Analysis

Time-dependent simulations were run, tracking both fluid field evolution and particle trajectories. The solution parameters included a two-phase time range: range (0,0.2,3.4) and range (3.5,0.02,7). Particle tracking with mass allowed for realistic tracing of tiny particles. The model formed after applying the geometrical condition at the beginning is shown in Figure 2. The Flow Pattern Resulting From Geometry is depicted in Figure 3.

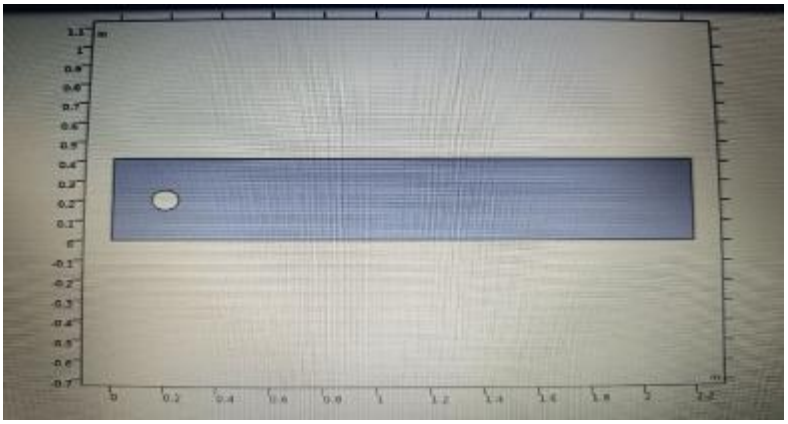

Figure 1 Model formed after applying the geometrical condition at the beginning

2.12. Step-by-Step Operation

- Software Initialization: COMSOL launched; Model Wizard set to 2D; Physics selection: Single Phase Flow – Laminar.
- Parameter Entry: Parameters (U_{mean}, H, W, R) and step function defined in Global Definition.
- Geometry Construction: Rectangle and circle created and combined via partitioning and difference operations to yield the desired domain.
- Material Specification: Blank material assigned; physical properties (density, viscosity) set accordingly.

2.13. Boundary Conditions

- Inlet: Parabolic velocity using a time-dependent step function.
- Outlet: Standard outlet boundary.
- Meshing: Physics-controlled, "finer" mesh generated, with boundary layer refinement near the cylinder.
- Time-Dependent Study Setup: Output times entered; intermediate solution steps enabled for stability.

2.14. Particle Tracing:

Initial velocities: x-component = u, y-component = v.

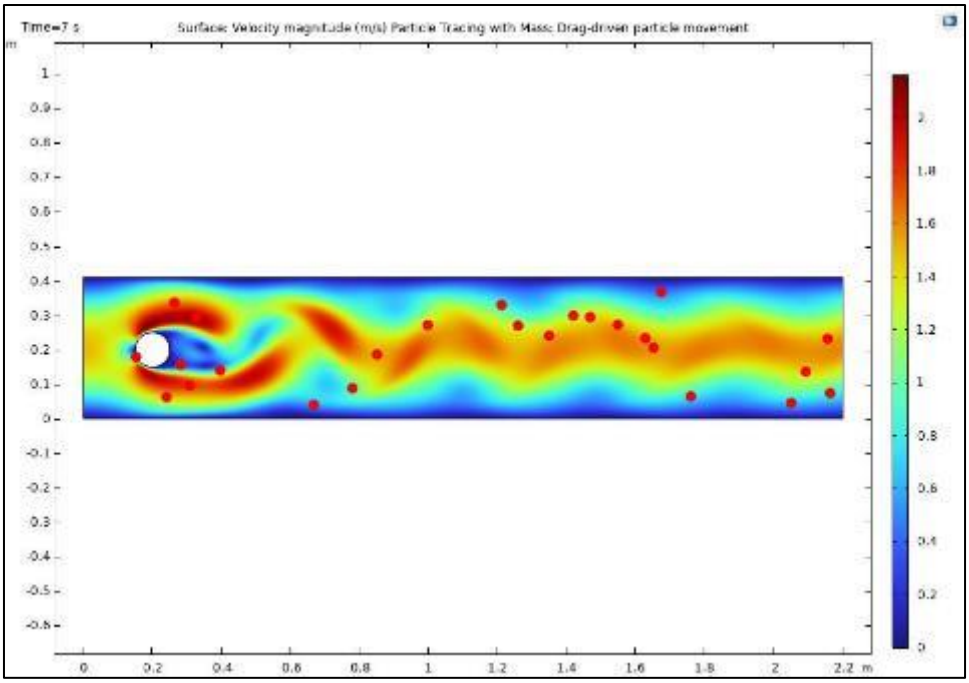

Figure 2 Flow Pattern Resulting From Geometry

- Particle release: Start time 3.6, interval 0.4, vertical range set for starting y positions.
- Particle motion: Disappear upon domain exit; style set to point.

2.15. Data Processing:

Integral evaluations are assigned along boundaries to calculate lift and drag coefficients.

1D plot groups established for each coefficient with expressions as above.

Visualization: Results plotted for particle paths and temporal profiles of lift and drag coefficients, completing the simulation workflow.

3. Results and Discussion

3.1. Lift-Coefficient (C_L)

A graph of lift coefficient (C_L) vs. time usually shows the variation of the lift coefficient over a given period of time, which can be simulated computationally or during an aircraft's flight. Lift-Coefficient with respect to time depicted in Figure 4.

3.2. Initial Steady-State Phase

At the beginning of the simulation, the lift coefficient remains nearly constant over time. This steady regime indicates that flow around the cylinder has reached a stable configuration, with minimal transient effects or disturbances. For particle-laden flows, this initial stability corresponds to uniform velocity and pressure fields near the cylinder before vortex shedding or significant wake development occurs.

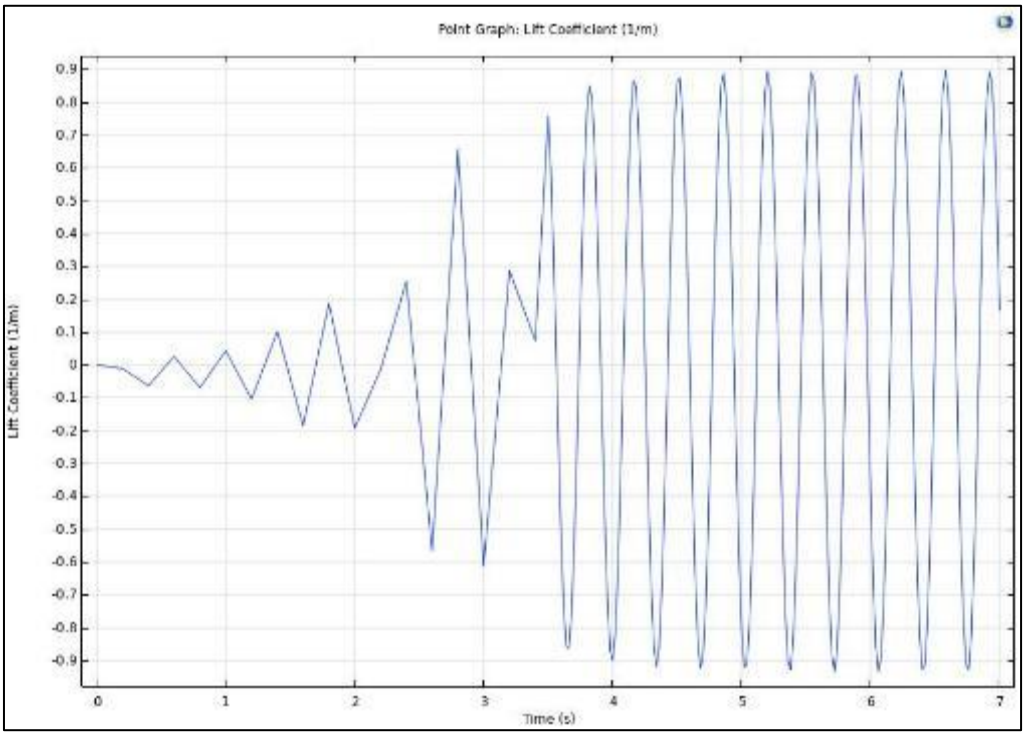

Figure 3 Lift-Coefficient with respect to time

3.3. Transitional (Transient) Phase

Following the initial steady state, the lift coefficient exhibits noticeable fluctuations. These transient oscillations are typically associated with the development of vortex structures in the cylinder wake. As the flow evolves, the interactions between shed vortices and the track of tiny particles introduce dynamic forces on the cylinder surface, resulting in time-dependent variations of the lift coefficient. This phase reflects the onset of unsteady flow and the sensitivity of lift generation to local instabilities and fluctuating flow conditions.

3.4. Sustained Constant-State Behavior

After the transient phase, the system often returns to a quasi-steady-state, where the lift coefficient stabilizes again, albeit sometimes at a different average value due to wake reorganization and sustained vortex shedding. In controlled simulations, this regime represents either the establishment of periodic vortex streets or statistically steady flow conditions. The lift coefficient in this phase characterizes the aerodynamic force due to stabilized, repetitive flow patterns and is directly influenced by particle distribution in the wake.

3.5. Influence of Parameter Variation and Controlled Inputs

Distinct step changes or pronounced shifts in the lift coefficient may be observed during periods where boundary conditions or model parameters, such as inlet velocity, particle release timing, or geometry, are altered. These step-like features on the coefficient graphs reveal the sensitivity of flow dynamics to control inputs and experimental perturbations, such as abrupt changes in inflow velocity or adjustment of particle numbers.

3.6. Terminal Phase and Overall Trends

Toward the end of the simulation, either a return to steady lift coefficient values or gradual transitions may appear, depending on whether the system re-stabilizes or external conditions continue to vary. This phase reflects the ability of the flow to restore stability or adjust to progressively changing boundary conditions. The overall time-dependent graph of the lift coefficient thus provides valuable insights into the flow's aerodynamic performance, stability, and the impact of dynamic events or controlled changes on force production. In summary, the temporal evolution of the lift coefficient in this COMSOL-based study elucidates the main phases of flow past a cylinder: initial stabilization, transient vortex evolution, re-establishment of periodicity, and response to model variations. These findings help interpret particle-fluid interactions and aerodynamic forces under practical laboratory and engineering scenarios.

3.7. Drag Coefficient (C_D) Analysis

The temporal variation of the drag coefficient (C_D) provides insight into the underlying flow dynamics as fluid passes around the cylinder. Drag coefficient as a function of time is depicted in Figure 5.

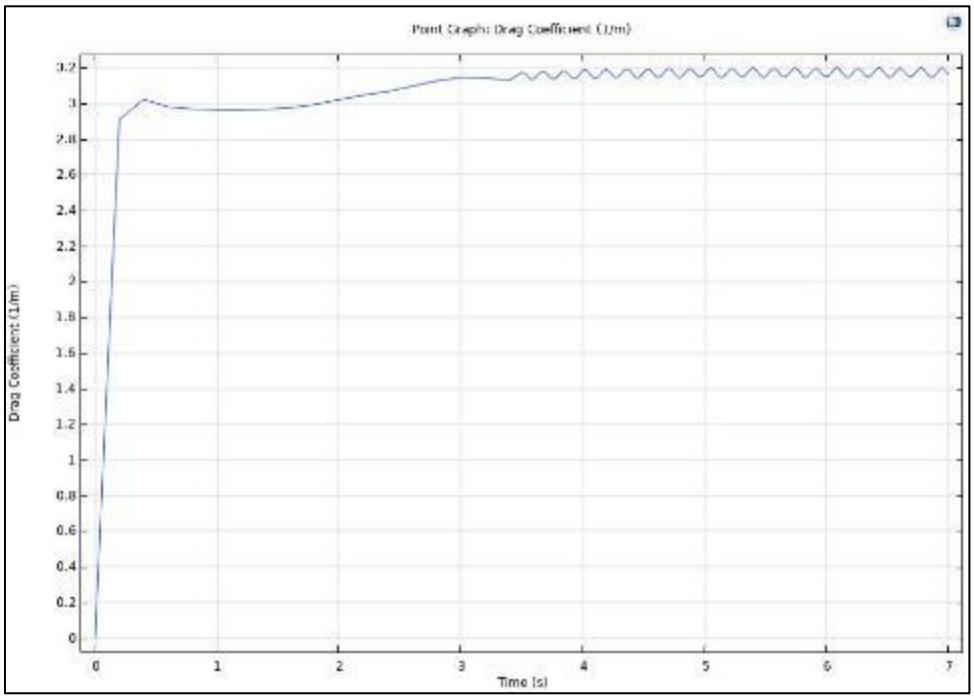

Figure 4 Drag coefficient as a function of time

The plot of CDC_DCD as a function of time (Figure 6.2) typically exhibits distinct behaviors depending on the flow regime and system characteristics. In steady-state laminar conditions, after the initial transients subside, CDC_DCD stabilizes and remains nearly constant. This reflects a fully developed wake and consistent drag force, often resulting in a flat horizontal trend in the CDC_DCD vs. time graph after the early adjustment period. Such behavior is commonly observed when the inflow velocity and system geometry do not change significantly over time. With the onset of unsteady flow

phenomena—such as flow instabilities, vortex shedding, or transition to turbulence—oscillations and fluctuations become evident in the CDC_DCD curve. These time-dependent variations correspond to periodic changes in the wake structure, leading to dynamic shifts in the drag forces acting on the cylinder. In simulations or experiments designed to capture these instabilities, CDC_DCD may reveal regular oscillations or more irregular, chaotic patterns if flow transitions are rapid.

In dynamically changing systems, such as those where the cylinder's orientation or velocity varies, CDC_DCD will mirror these adjustments, displaying either gradual or abrupt changes over time. This dynamic response demonstrates the sensitivity of drag force to both flow and boundary conditions. Both computational and experimental studies utilize these CDC_DCD versus time graphs to quantify the stability of flow regimes and identify transition points between laminar and turbulent states. In some results, the variation in CDC_DCD may be shaded or accompanied by error bars to illustrate inherent uncertainties or fluctuations due to physical or numerical factors. Overall, the CDC_DCD versus time graph does not have a universal pattern but instead reflects the fluid's dynamic interactions with the solid boundary under the prescribed system conditions.

3.8. Separation of the Boundary Layer

Whenever a solid body is immersed in a flowing fluid, a boundary layer—an extremely thin region adjacent to the solid surface—forms due to viscosity. Within this layer, the fluid velocity increases from zero (at the solid surface, due to the no-slip condition) to the free stream value. As the fluid progresses along the surface of the cylinder, the boundary layer's thickness grows. This growth is dictated by the need for the fluid in the boundary layer to continually supply kinetic energy to overcome viscous resistance at the wall. As a result, there is a gradual reduction in momentum within the fluid elements nearest the surface, compensated by momentum transfer from fluid just outside the boundary layer. However, as the fluid moves further downstream, especially in regions where the pressure increases along the direction of flow (an adverse pressure gradient), the boundary layer may be deprived of sufficient kinetic energy to maintain attachment to the surface. When this energy deficit is reached, the boundary layer can no longer adhere and separates from the body. The point at which the boundary layer detaches is known as the separation point. The occurrence and location of separation are governed by the interplay between increasing flow velocity (resulting in a decrease in pressure, i.e., a favorable pressure gradient) and any sudden reductions in velocity (producing an adverse pressure gradient, which promotes separation). A clear understanding of these gradients is essential for interpreting wake formation, drag fluctuations, and the efficiency of particle transport around immersed bodies.

4. Conclusion

The study successfully demonstrated the application of COMSOL Multiphysics 6.1 for simulating the flow of tiny particles past a circular cylinder in laminar and transitional regimes. The coupled analysis of fluid dynamics and particle trajectories provided detailed insights into wake formation, vortex shedding, and drag coefficient behavior over time. The simulation results illustrated how the drag coefficient varied under steady and unsteady flow conditions, correlating well with boundary layer separation phenomena observed in classical fluid mechanics. The study highlighted the critical influence of flow parameters and particle properties on hydrodynamic forces and particle transport patterns. By incorporating realistic fluid-solid interactions through multiphysics modeling, this work contributes a valuable computational framework for predicting microscale particle behavior in engineering applications. Future work could extend this approach to turbulent flows and three-dimensional configurations, as well as explore particle interactions and multiphase couplings for enhanced fidelity. Overall, the findings emphasize the importance of rigorous numerical modeling for optimizing designs and controlling flows involving particulate matter around cylindrical bodies.

Compliance with ethical standards

Acknowledgement

The authors gratefully thank faculties and staff of Mechanical Department of Engineering, for their supports.

Disclosure of conflict of interest

No conflict of interest to be disclosed.

References

[1] Ullah, I., Arif, M., Nadeem, S., & Alzabut, J. (2024). Numerical computations of MHD mixed convection flow of Bingham fluid in a porous square chamber with a wavy cylinder. International Journal of Thermofluids, 24, 100938.

[2] Jiang, H., & Cheng, L. (2021). Large-eddy simulation of flow past a circular cylinder for Reynolds numbers 400 to 3900. Physics of Fluids, 33(3).

[3] Wang, J., Ma, L., Jiang, M., Fang, Q., Yin, C., Tan, P., ... & Chen, G. (2024). Direct numerical simulation of the drag, lift, and torque coefficients of high aspect ratio biomass cylindrical particles. Physics of Fluids, 36(1).

[4] Braza, M., Chassaing, P., & Ha Minh, H. (1986). Numerical study and physical analysis of the pressure and velocity fields in the near wake of a circular cylinder. Journal of Fluid Mechanics, 165, 79-130.

[5] Rodi, W. (1991). Experience with two-layer models combining the k-epsilon model with a one-equation model near the wall. In 29th Aerospace Sciences Meeting, 216.

[6] Achenbach, E., & Heinecke, E. (1981). On vortex shedding from smooth and rough cylinders in the range of Reynolds numbers 6×103 to 5×106. Journal of Fluid Mechanics, 109, 239-251.

[7] Williamson, C. H. K. (1996). Vortex dynamics in the cylinder wake. Annual Review of Fluid Mechanics, 28(1), 477-539.

[8] Norberg, C. (2003). Fluctuating lift on a circular cylinder: review and new measurements. Journal of Fluids and Structures, 17(1), 57-96.

[9] Sheridan, J., Lin, J. C., & Rockwell, D. (1997). Flow past a cylinder close to a free surface. Journal of Fluid Mechanics, 330, 1-30.

[10] Barkley, D., & Henderson, R. D. (1996). Three-dimensional Floquet stability analysis of the wake of a circular cylinder. Journal of Fluid Mechanics, 322, 215-241.

[11] Thompson, M. C., Hourigan, K., & Sheridan, J. (1996). Three-dimensional instabilities in the wake of a circular cylinder. Experimental Thermal and Fluid Science, 12(2), 190-196.

[12] Honji, H., Tatsuno, M., & Matsumoto, T. (1980). An experimental study of the flow around a circular cylinder near a plane surface. Fluid Dynamics Research, 2(2), 95-105.

[13] Reichl, P., Hourigan, K., & Thompson, M. C. (2005). Flow past a cylinder close to a free surface. Journal of Fluid Mechanics, 533, 269-296.

[14] Gopalan, S., & Katz, J. (2000). Flow structure and modeling issues in the closure region of attached cavitation. Physics of Fluids, 12(4), 895-911.

[15] Oshkai, P., & Rockwell, D. (1999). Free surface wave system generated by a horizontal cylinder. Journal of Fluids and Structures, 13(7-8), 935-954.

[16] Oliveira, P. J., Issa, R. I., & Ahmadi-Befrui, B. (1998). Computation of turbulent flows around a square cross-section cylinder using two-equation turbulence models. International Journal for Numerical Methods in Fluids, 28(8), 1181-1202.

[17] Koo, B., Yang, J., Yeon, S. M., & Stern, F. (2014). Reynolds and Froude number effect on the flow past an interface-piercing circular cylinder. International Journal of Naval Architecture and Ocean Engineering, 6(3), 529-561.

[18] Bouscasse, B., Colagrossi, A., Marrone, S., & Antuono, M. (2013). Nonlinear water wave interaction with floating bodies in SPH. Journal of Fluids and Structures, 42, 112-129.

[19] Lin, J. C., & Rockwell, D. (1999). Vortex formation from a cylinder in shallow water. Journal of Fluids and Structures, 13(6), 785-801.

[20] Lin, J. C., Ozgoren, M., & Rockwell, D. (2003). Space-time development of the onset of a shallow-water vortex. Journal of Fluid Mechanics, 485, 33-66.

[21] Nguyen, T. D., Pham, D. C., & Ngo, T. D. (2020). Numerical study of flow around a circular cylinder using COMSOL Multiphysics. IOP Conference Series: Materials Science and Engineering, 869(3), 032016.

[22] Rajani, B. N., Kandasamy, A., & Majumdar, S. (2009). Numerical simulation of laminar flow past a circular cylinder. Applied Mathematical Modelling, 33(3), 1228-1247.

[23] Kim, D., Park, J., & Choi, H. (2018). Dynamic coupling of fluid-structure interaction in vortex-induced vibration. Journal of Fluids and Structures, 76, 593-615.

[24] Cao, S., Ozono, S., Tamura, Y., Ge, Y., & Kikugawa, H. (2010). Numerical simulation of Reynolds number effects on velocity shear flow around a circular cylinder. Journal of Fluids and Structures, 26(5), 685-702.

[25] Kim, D., Park, J., & Choi, H. (2018). Dynamic coupling of fluid-structure interaction in vortex-induced vibration. Journal of Fluids and Structures, 76, 593-615.

[26] Rashidi, S., Hayatdavoodi, M., & Esfahani, J. A. (2016). Vortex shedding suppression and wake control: A review. Ocean Engineering, 126, 57-80.

[27] Zhang, C., Li, Y., & Meng, Q. (2021). Machine learning in computational fluid dynamics: Prediction of drag forces on circular cylinders. Ocean Engineering, 221, 108550.